G9a inhibition promotes the formation of pacemaker-like cells by reducing the enrichment of H3K9me2 in the HCN4 promoter region

PEI XU[1*], KAI JIN[2*], JING ZHOU[3*], JIANGUN GU[4], XIANG GU[4], LIJUAN DONG[4] and XIAOLIN SUN[2]

Departments of [1]Haematology and [2]Cardiology, Taizhou People's Hospital, Taizhou, Jiangsu 225300; [3]College of Animal Science and Technology, Yangzhou University; [4]Department of Cardiology, Northern Jiangsu People's Hospital, Yangzhou, Jiangsu 225001, P.R. China

Received June 14, 2022; Accepted November 4, 2022

DOI: 10.3892/mmr.2022.12908

Abstract. Biological pacemakers, made of pacemaker-like cells, are promising in the treatment of bradyarrhythmia; however, the inefficiency of stem cell differentiation into pacemaker-like cells has limited their clinical application. Previous studies have reported that histone H3 at lysine 9 (H3K9) methylation is widely involved in the proliferation and differentiation of cardiomyocytes, but the specific role of H3K9 dimethylation (H3K9me2) in the formation of pacemaker cells remains unclear. The present study evaluated the functional role of H3K9me2 in the differentiation of bone marrow mesenchymal stem cells (BMSCs) into pacemaker-like cells. Rat BMSCs pretreated with the euchromatic histone lysine methyltransferase 2 (G9a) inhibitor BIX01294 were transfected with a T-box 18 overexpression plasmid to induce BMSCs to form pacemaker-like cells. The induced pacemaker-like cells were analyzed using reverse transcription-quantitative PCR (RT-qPCR) and immunofluorescence to assess the efficiency of differentiation. The enrichment of H3K9me2 in the hyperpolarized-activated cyclic nucleotide-gated cation channel (HCN)4 promoter region was assessed by chromatin immunoprecipitation (ChIP). In addition, BIX01294 was injected into rats, and the protein and mRNA expression levels of HCN4 were assessed using western blotting and RT-qPCR. After interference with G9a using BIX01294, ChIP results demonstrated that H3K9me2 levels in the promoter region of HCN4 were markedly decreased. Immunofluorescence and RT-qPCR demonstrated that the protein expression levels of certain cardio-specific proteins in the treated group were significantly higher compared with those in the untreated group. *In vivo* experiments demonstrated that interference with G9a could cause pathological hypertrophy. Furthermore, *in vitro* and *in vivo* inhibition of G9a could increase the differentiation and proliferation of pacemaker-like cells by decreasing the levels of H3K9me2 in the promoter region of HCN4 gene.

Correspondence to: Dr Xiaolin Sun, Department of Cardiology, Taizhou People's Hospital, 366 Taihu Road, Taizhou, Jiangsu 225300, P.R. China
E-mail: sunxiaolin19@sina.cn

*Contributed equally

Key words: histone H3 at lysine 9, euchromatic histone lysine methyltransferase 2, pacemaker-like cells, hyperpolarized-activated cyclic nucleotide-gated cation channel 4, promoter region

Introduction

Bradycardia, including pathological sinus syndrome and atrioventricular block, is a serious threat to human life. Compared with electronic pacemakers, which have numerous defects, biological pacemakers have a promising application in the treatment of bradyarrhythmia (1). However, it is inefficient to induce stem cells to differentiate into pacemaker cells *in vitro*; therefore, the mechanism of pacemaker cell differentiation needs to be elucidated (2).

The T-box (Tbx) gene family, including Tbx3 and Tbx18, serves an important role in the formation of the sinoatrial node. Tbx18-mediated phenotypic transformation of bone marrow mesenchymal stem cells (BMSCs) into pacemaker-like cells has been reported at both the mRNA and protein levels (3-5). *In vivo*, it has been reported that Tbx18 can directly reprogram cardiomyocytes into sinoatrial node-like cells, increase the expression of hyperpolarized-activated cyclic nucleotide-gated cation channel (HCN)4 on the membrane and thus improve the beating frequency of the cell (6,7). However, the differentiation efficiency of pacemaker-like cells is still not high and only ~7% of BMSC-Tbx18 cells were reported to beat on day 10 after transfection with a Tbx18 overexpression vector (8). Therefore, the present study assessed a potential new method to improve the efficiency of differentiation of BMSCs into pacemaker-like cells.

Previous studies have reported that histone H3 at lysine 9 dimethylation (H3K9me2) is closely related to cell differentiation, proliferation and reprogramming. It has been reported that regulation of the expression of H3K9me2 during cardiomyocyte maturation can affect the expression of cardiac development-related genes (9). Furthermore, the euchromatic

histone lysine methyltransferase 2 (G9a) inhibitor BIX01294 can increase the number of cardiac progenitor cells without impairing their differentiation ability, which suggests that the drug may have the effect of producing a large number of cardiac progenitor cells for cardiac repair (10). Moreover, after BIX01294 pretreatment, the levels of cardiomyocyte markers GATA4, Nkx2.5 and myocardin produced by Wnt11 factor-induced mesenchymal stem cells were reported to be 2.6-5.6x higher than those in the untreated group (9,11). These studies indicated that G9a may participate in the development of cardiomyocytes.

In the present study, to increase the efficiency of pacemaker-like cell formation, BMSCs treated with BIX01294 were induced to form pacemaker-like cells by overexpression of Tbx18. The present study optimized the efficiency of pacemaker-like cell induction *in vitro*, which may lay the foundation for clinical application.

Materials and methods

BMSCs isolation and cell culture. A total of 20 healthy male and 20 healthy female Wistar rats (weight, 50-200 g; age, 3-8 weeks) were provided by Yangzhou University (Yangzhou, China) and three female or male rats were used in each of three individual experiments of BMSCs isolation and cell culture. Rats received standard care under a 12-h dark/light cycle (25˚C with humidity of 60%), and were given free access to food and water. Before the experiment, adaptive feeding was performed for 1 week. The health and behavior of the animals were monitored daily until death. All procedures involving the care and use of animals conformed to the Animal Research: Reporting of *In Vivo* Experiments (ARRIVE guidelines 2.0; https://arriveguidelines.org/arrive-guidelines) and were approved by the Laboratory Animal Management and Experimental Animal Ethics Committee of Yangzhou University (approval no. 202003545). All rats were anesthetized using 20% sodium urethane (0.2 g/ml; 1.0 g/kg; intraperitoneal injection) and were subsequently sacrificed by cervical dislocation. Animal death was verified by ascertaining cardiac and respiratory arrest. Bone marrow cells were extracted from the tibia and femur. The bone marrow liquid was centrifuged at 1,100 x g for 10 min at 37˚C and the supernatant was discarded. The cell suspension was transferred to a 15 ml centrifuge tube containing 5 ml Percoll (1.073 g/ml; Sigma-Aldrich; Merck KGaA). Cells were dispersed by pipetting again and centrifuged at 1,500 x g for 30 min at 4˚C. The mononuclear cells in the middle layer were obtained. After washing with phosphate-buffered saline (PBS), the cells were resuspended in low-glucose DMEM (Thermo Fisher Scientific, Inc.) containing 20% FBS (Biowest) and 100 U/ml penicillin/streptomycin , and then inoculated in the culture plate. The cells were cultured in a 5% CO_2 incubator at 37˚C for 72 h and then half the solution replaced. During the expansion and proliferation of MSCs, the culture medium was replaced every three days and cells were passaged once they reached 80% confluency. After that, the culture medium was passed every ~3 days and third-generation cells were collected for subsequent experimental use. Bone marrow mesenchymal stem cells grow adherent to the wall, and cellular morphological feature exhibiting a spindle shape.

Flow cytometry. For cell phenotypic characterization, BMSCs from the third passage were stained using mouse anti-CD29 (1:100; cat. no. sc-9970; Santa Cruz Biotechnology, Inc.), anti-CD34 (1:100; cat. no. sc-7324; Santa Cruz Biotechnology, Inc.), anti-CD44 (1:100; cat. no. sc-7297; Santa Cruz Biotechnology, Inc.) and anti-CD45 (1:100; cat. no. sc-1178; Santa Cruz Biotechnology, Inc.) antibodies for 1 h at room temperature. Phycoerythrin A-labeled anti-mouse IgG (1:100; cat. no. sc-516141; Santa Cruz Biotechnology, Inc.) was used as the secondary antibody for 1 h at room temperature. After washing with PBS, flow cytometry was performed using a BD FACSCalibur (BD Biosciences). The results were analyzed and processed by FlowJo version 10.0 (FlowJo LLC).

Construction of the Tbx18 lentiviral vector and cell transduction. According to the Tbx18 sequence accessed from the National Center for Biotechnology Information, primers for full-length expression of the CDS region were designed as follows: Forward, 5'-TATAGGGAGACCCAAGCTGGA TGGCGGAGAAGCGGAGG-3' and reverse 5'-CGGGCC CTCTAGACTCGAGCTCAGACCATATGCGCAGACAC-3'. T4 ligase was used to connect the CDS with the pcDH-CMV-MCS-EF1-TAGFP + Puro vector from our laboratory, which was digested using *Not*I and *Nhe*I to construct the Tbx18 overexpression plasmid (OE-Tbx18). The plasmid was sent to Shanghai TsingKE Biologicals for Sanger sequencing for verification of the construct. After sequencing, OE-Tbx18 was sent to Jiman Biotechnology (Shanghai) Co., Ltd. for lentiviral packaging (titer: $2.5x10^8$ TU/ml).

BMSCs were plated in 24-well plates, grown to 70-80% confluence and transfected using 1 μg/plate OE-Tbx18 and 6 μg/ml polybrene. Cells not transfected with plasmids were used as controls. BMSCs transfected, according to the same protocol as OE-Tbx18, with a no-load vector were the negative control. After incubation at 37˚C for 24 h, the virus-containing medium was replaced with fresh medium. Continue incubation for 48 h, the cells were observed daily using a TE2000 fluorescence microscope (magnification, x100, x200 and x400; Nikon Corporation). The beating rate of 100 cells was assessed three times each day during 3 consecutive days after 10 days.

Immunofluorescence and immunohistochemistry (IHC). BMSCs were fixed using 4% paraformaldehyde at 4˚C for 30 min. Fixed cells were permeabilized using 0.1% Triton X-100 (Beijing Solarbio Science & Technology Co., Ltd.) and blocked using 2% FBS (Biowest) and 0.1% Tween-20 (Beijing Solarbio Science & Technology Co., Ltd.) blocking solution at 4˚C for 2 h. The cells were then incubated overnight at 4˚C with primary antibody against rat cardiac troponin I (cTnI; 1:200; cat. no. 21652-1-AP; ProteinTech Group, Inc.). Cells stained with diluent only served as the negative control. After overnight incubation, cells were washed with PBS three times (5 min/wash), incubated with Cy3-conjugated secondary antibody (1:500; cat. no. A0516; Beyotime Institute of Biotechnology) for 1 h at room temperature and washed five times with PBS. Nuclei were stained using 4',6-diamidino-2-phenylindole (Beijing Solarbio Science & Technology Co., Ltd.) for 10 min at room temperature. Slides were mounted and assessed using a TE2000 fluorescence microscope.

Table I. Sequences of primers used for reverse transcription-quantitative PCR.

Gene	Sequence (5'-3')	Accession number
cTnI	F: GCCGGAAGTGTAGGAAGA R: GGGGAGCAGATGATGGT	NM_012676.1
Nppa	F:TGCCGGTAGAAGATGAGGT R: GTTGACTTCCCCAGTCCAG	NM_012612.2
Nppb	F: ATTCTGCTCCTGCTTTTCC R: GCTTCTGCATCGTGGATT	NM_031545.1
Myh7	F: ATTGCCGAGTCCCAGGT R: TCCAGGTCTCAGGGCTTC	NM_017240.2
HCN4	F: CAGCCAGAAAGCAGTGGA R: ATCAGCAACAGCATCGTCA	NM_021658.1
Tbx18	F:CCCGTGGACAACAAAAGA R: CGGTGAGTCTGGATGAATG	NM_001108173.1
α-SA	F:TGGCATCTGAATGGGTCT R: CAGTGGGTTCTTGGCTTC	NR_045097.1
GAPDH	F: GGAAAGCTGTGGCGTGATGG R: GTAGGCCATGAGGTCCACCA	NM_017008.4

cTnI, cardiac troponin I; Nppa, natriuretic peptide A; Nppb, natriuretic peptide B; Myh7, myosin heavy chain 7; HCN4, hyperpolarization-activated cyclic nucleotide-gated channel 4; Tbx18, T-box 18; α-SA, α-striated actin; F, forward; R, reverse.

The rat heart tissue were collected for IHC staining. The tissue sections were dewaxed, hydrated, incubated in citrate buffer for antigen retrieval and fixed, then blocked in TBS-0.05% Tween 20 containing 5% BSA. Tissue sections were incubated with anti-G9a (1:300; cat. no. sc-515726; Santa Cruz Biotechnology, Inc.), anti-HCN4 (1:200; cat. no. ab289962; Abcam, Inc.) at 4˚C overnight, washed in TBST three times for 10 min and then incubated with secondary antibodies; anti-rabbit (1:400, cat. no. ab150081; Abcam, Inc.) and biotinylated anti-mouse (1:400, cat. no. B7401; Sigma-Aldrich; Merck KGaA) for 2 h at room temperature and tertiary antibodies (streptavidin-HRP; cat. no. 18-152; Sigma-Aldrich; Merck KGaA) to label targets with HRP, incubated for 30 sec-1 min with DAB (cat. no. 11718096001; Sigma-Aldrich; Merck KGaA) substrate. Slides were counterstained with hematoxylin for 2 min at room temperature and coverslips were added before imaging.

Reverse transcription-quantitative PCR (RT-qPCR). Total RNA was extracted from the BMSCs of different treatment groups and cardiomyocytes (CM) using TRIzol® (Invitrogen; Thermo Fisher Scientific, Inc.) and cDNA was synthesized from sample RNA using FastKing One Step RT-qPCR kit Qiagen GmbH. The amplification steps included 50˚C 10 min, 95˚C 3 min, 95˚C 15 sec and 60˚C 30 sec for 40 cycles. cDNA was amplified by qPCR using a Qiagen PCR kit (Qiagen GmbH) according to the manufacturer's protocols at 50˚C for 30 min, 95˚C for 3 min, 95˚C for 15 sec and 60˚C for 30 sec. The mRNA expression levels of Tbx18, α-1 antitrypsin (α-SA), cTnI, HCN4, and the pathological hypertrophy marker genes natriuretic peptide A (Nppa), natriuretic peptide B (Nppb) and myosin heavy chain 7 (Myh7) were assessed using qPCR. The 20 μl PCR amplification reaction included 2 μl cDNA, 10 μl SYBR Taq, 0.8 μl forward primer, 0.8 μl reverse primer, 0.4 μl RoxII and 6 μl double-distilled water. PCR was performed on the basis of the two-step procedure (95˚C for 15 min; 95˚C for 10 sec and 60˚C for 32 sec) repeated 40 times. The primer sequences used are presented in Table I. The PCR instrument used for qPCR was an ABIPRISM 7500 (Applied Biosystems; Thermo Fisher Scientific, Inc.). Each experimental condition was repeated in triplicate. Each experiment was repeated three times. The relative mRNA expression levels were quantified using the $2^{-\Delta\Delta Cq}$ method (9,12), and normalized to GAPDH.

Western blotting. Total protein was extracted from BMSCs and myocardial tissue using RIPA lysis buffer (cat. no. R0010; Beijing Solarbio Science & Technology Co., Ltd.) on ice for 30 min. Total protein concentrations were evaluated using a protein assay kit (Beyotime Institute of Biotechnology). The protein samples (10 μg/lane) were then separated using 10% SDS-PAGE and electrophoresed. The proteins were electro-transferred onto PVDF membranes. Subsequently, the membranes were blocked for 2 h at room temperature in TBS-0.05% Tween 20 containing 5% nonfat milk. Primary antibodies against H3K9me2 (1:1,000; cat. no. 39239; Active Motif, Inc.), H3 (1:3,000; cat. no. H0164; Sigma-Aldrich; Merck KGaA), G9a (1:1,000; cat. no. sc-515726; Santa Cruz Biotechnology, Inc.), Nappa (1:1,000; cat. no. 13299-1-AP; ProteinTech Group, Inc.), Nappb (1:1,000; cat. no. 27426-1-AP; ProteinTech Group, Inc.), Myh7 (1:1,000; cat. no. 22280-1-AP; ProteinTech Group, Inc.), β-actin (1:1,000; cat. no. SAB3500350; Sigma-Aldrich; Merck KGaA), HCN4 (1:1,000; cat. no. 55224-1-AP; ProteinTech Group, Inc.), cTnI (1:1,000; cat. no. 21652-1-AP; ProteinTech Group, Inc.), α-SA (1:1,000; cat. no. 23660-1-AP; ProteinTech Group, Inc.) and Tbx18 (1:1,000; cat. no. 23237-1-AP; ProteinTech

Group, Inc.) were incubated with the membranes overnight at 4˚C. Finally, the membranes were incubated with the corresponding secondary antibodies (1:3,000, cat. no. A9169; 1:5,000, cat. no. AP160P; both Sigma-Aldrich; Merck KGaA). for 2 h at room temperature and assessed using an ECL Chemiluminescent Substrate Reagent Kit (Thermo Fisher Scientific, Inc.). H3 is used as loading control to detect H3K9me2. Densiometric analysis was performed using Image Lab software (version 3.0, Bio-Rad Laboratories, Inc.).

Chromatin immunoprecipitation (ChIP)-qPCR analysis. BMSCs treated with BIX01294 at day 10 were collected and crosslinked using 1% formaldehyde at 37˚C for 10 min followed by glycine un-crosslinking. SDS lysis solution (Applygen Technologies, Inc.) was used to lyse the cells and the DNA was sonicated on ice to fragmentation for 5 sec with 10 sec intervals in a cycle lasting 5 min followed by centrifugation at 12,000 x g for 10 min at 4˚C, The supernatant was collected and incubated overnight at 4˚C on a shaker with 60 μl of Protein A/G Agarose in equal volumes and anti-H3K9me2 (cat. no. 39239; Active Motif, Inc.). The immunoprecipitation complexes are washed sequentially as follows: Low salt wash buffer (one wash), high salt wash buffer (one wash), LiCl wash buffer (one wash) and TE buffer (two washes). Elution buffer (120 μl) was added to each group to elute DNA, incubated for 15 min and centrifuged at 2,000 x g for 1 min at room temperature to collect the supernatant. NaCl (20 μl of 5 M; final NaCl concentration of 0.2 M) was added to each group, mixed well and uncrosslinked at 65˚C overnight. Tthe DNA was purified and recovered, and RT-qPCR was performed according to the aforementioned method. Specific steps were performed according to the manufacturer's protocol for the Chromatin Immunoprecipitation (ChIP) Assay kit (MilliporeSigma). In these experiments, 'input' was used to indicate the total protein, the percentage of its protein content bound by the IgG antibody (1:1,000; cat. no. HA1001; HUABIO, Inc.) was used as the 'control' and the percentage of protein bound by the target antibody was used as the 'experimental group'.

Animal experiment. A total of 20 Wistar rats (10 male and 10 female; age, 3-4 weeks; weight, 70±10 g) were randomly divided into two groups as follows: Treatment group and control group. The housing, handling and euthanasia procedures were the same as the aforementioned methods for BMSCs isolation. The tails of all rats were washed with warm water and wiped with 75% alcohol cotton ball for disinfection. Rats in the treatment group were injected with BIX01294 (10 mg/kg/day; MedChemExpress, Inc.) through the tail vein from day 1 to day 10 and rats in the control group were injected with normal saline. All of the rats were sacrificed for cardiac tissue collection at day 50.

Hematoxylin and eosin (H&E) staining. The sinus nodal region tissue was fixed in 4% paraformaldehyde for 24 h at room temperature. After dehydration using an ascending ethanol series, xylene was used as a clearing agent, and the tissues were embedded in paraffin and sectioned (5-6 μm). The slices were dewaxed using xylene, hydrated using a descending ethanol series at room temperature, then stained with hematoxylin (0.4%) and eosin (0.1%) (H&E) solution at 37˚C for 5 min, dehydrated using a rising ethanol series and neutral resin sealed at room temperature. The sections were assessed using a light microscope (Leica Microsystems GmbH).

Statistical analysis. The results are presented as the mean ± standard error of the mean. Data were assessed using one-way ANOVA and Tukey's post hoc test using SPSS 23 (IBM Corp). GraphPad Prism 7.0 GraphPad Software, Inc. was used for graph generation. Each test was evaluated at the 0.05 alpha level and $P<0.05$ was considered to indicate a statistically significant difference.

Results

Characteristics of BMSCs and transfection efficiency. To obtain rat BMSCs, the cells collected by density gradient centrifugation were cultured for 48 h. Certain adherent cells that grew in a spindle shape could be seen under the microscope and a few cells were polygonal. After 7-10 days, the fusion rate of cells, which were arranged in a swirling pattern, grew to 80-90% (Fig. 1B). The expression of surface markers of BMSCs were assessed and the proportion of cells positive for CD29 and CD44 expression were 96.34±3.15 and 81.64±3.26%, respectively, whereas the proportion of cells positive for CD34 and CD45 were only 0.28±0.12 and 1.28±0.43%, respectively (Fig. 1A), which was consistent with previously reported results (13). These results indicated that BMSCs were successfully isolated. When the cell fusion rate reached 80%, cells were transfected with the target vector and empty vector. Red fluorescence was assessed 24 h after transfection (Fig. 1C). After 72 h of transfection, western blotting and RT-qPCR revealed that the protein and mRNA expression levels of Tbx18 were significantly increased compared with those in the control group (Fig. 1E and F), which indicated that the OE-Tbx18 vector was successfully transfected into BMSCs (BMSCs-Tbx18).

Tbx18 overexpression in BMSCs promotes BMSCs differentiation into pacemaker-like cells. To evaluate whether overexpression of Tbx18 could enable BMSCs to differentiate into pacemaker-like cells, the cells were assessed using a microscope, which demonstrated morphological changes in the BMSCs 10 days after transfection (Fig. 1D). The spindle-shaped BMSCs transformed into strips, which was a typical feature of sinoatrial node cells. Furthermore, ~5% of BMSCs-Tbx18 were observed to be beating at day 10. Immunofluorescence demonstrated that certain cells expressed cTnI (Fig. 2A). Cardiomyocyte was used as a positive control, the mRNA and protein expression levels of α-SA, cTnI and HCN4 were significantly increased in BSMCs-Tbx18 compared with in the control group, as determined using RT-qPCR and western blotting (Fig. 2B and C). These results demonstrated that overexpression of Tbx18 promoted BMSCs differentiation into pacemaker-like cells.

G9a inhibition stimulates the expression of HCN4 sequences in BMSCs. To evaluate the effect of G9a on the differentiation of BMSCs into pacemaker-like cells, the OE-Tbx18 was transfected into BMSCs after treatment with 1 μM BIX01294 for 12 h. Western blotting demonstrated that the protein

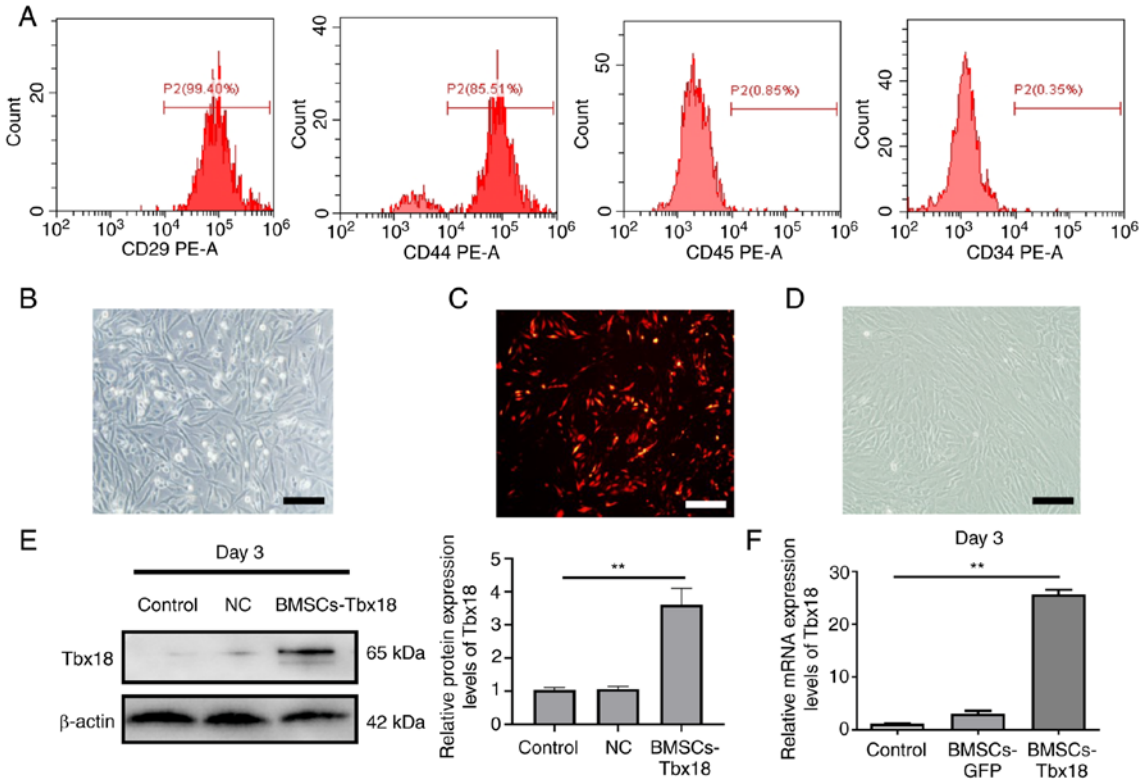

Figure 1. Characteristics of BMSCs and transfection efficiency. (A) Fluorescence-activated cell sorting analysis of CD29, CD44, CD34 and CD45 protein expression levels in BMSCs. (B) Cellular morphological features of BMSCs, which exhibited a spindle shape. Scale bar, 50 μm. (C) Red fluorescence of BMSCs after transfection with OE-Tbx18 for 48 h. Scale bar, 50 μm. (D) The microscopic morphology of BMSCs gradually evolved into strip-like features after 10 days of transduction by OE-Tbx18. Scale bar, 50 μm. (E) Western blotting of Tbx18 protein expression levels after transfection for 72 h. BMSCs without transfection were used as the control, BMSCs transfected with the empty vector were used as the NC. (F) Reverse transcription-quantitative PCR analysis of Tbx18 mRNA expression levels after transfection for 72 h. **P<0.01. BMSCs, bone marrow mesenchymal stem cells; OE-Tbx18, T-box 18 overexpression plasmid; NC, negative control.

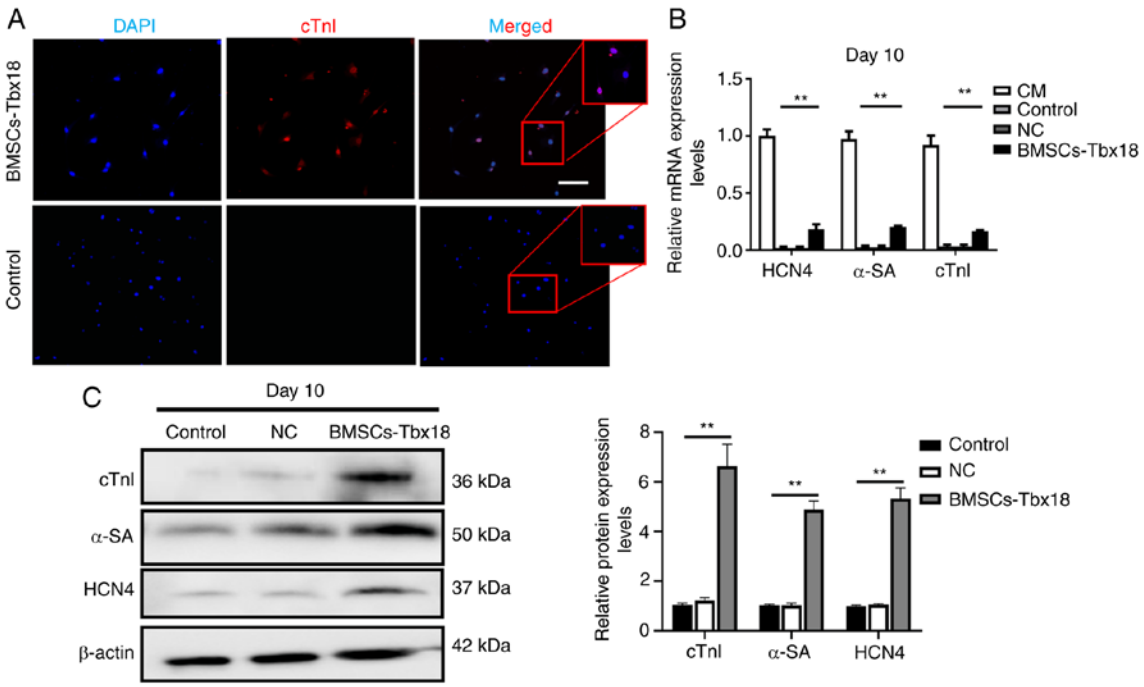

Figure 2. Immunostaining, western blotting and reverse transcription-quantitative PCR analysis of target protein and mRNA expression levels after transfection. (A) Protein expression levels of cTnI in BMSCs were assessed using immunostaining with cTnI-specific primary antibodies and a Cy3 secondary antibody. Scale bar, 50 μm. (B) Quantitative analysis of the relative mRNA expression levels of HCN4, α-SA and cTnI. (C) Western blotting demonstrated increased HCN4, α-SA and cTnI protein expression levels. BMSCs without transfection were used as the control and BMSCs transfected with the empty vector were used as the NC. **P<0.01. cTnI, cardiac troponin I; HCN4, hyperpolarization-activated cyclic nucleotide-gated channel 4; α-SA, α-striated actin; NC, negative control; CM, cardiomyocyte; BMSCs, bone marrow mesenchymal stem cells.

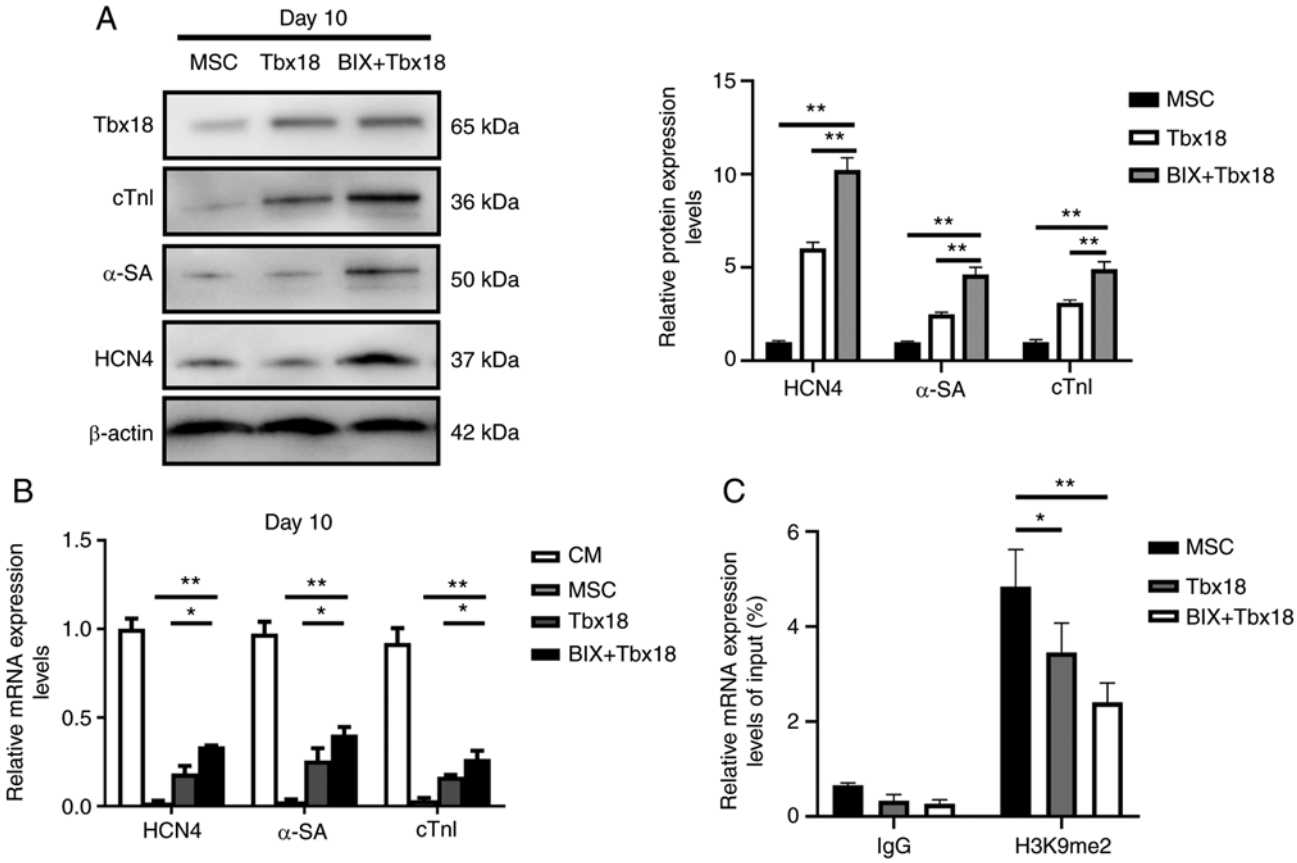

Figure 3. Expression of target protein after G9a inhibition treatment. (A) Western blotting demonstrated increased HCN4, α-SA and cTnI protein expression levels in different groups. (B) Quantitative analysis of the mRNA expression levels of HCN4, α-SA and cTnI. (C) Chromatin immunoprecipitation-qPCR analysis for H3K9me2 binding to the HCN4 promoter. The histogram showed the amount of immunoprecipitated DNA as detected using the qPCR assay. Values are indicated as % of input. *P<0.05 and **P<0.01. cTnI, cardiac troponin I; HCN4, hyperpolarization-activated cyclic nucleotide-gated channel 4; α-SA, α-striated actin; CM, cardiomyocyte; BIX, H3K9me2, histone H3 at lysine 9 dimethylation; Tbx18, T-box 18 overexpression plasmid.

expression levels of α-SA, cTnI and HCN4 in BMSCs treated with BIX01294 (BIX-BMSCs) were significantly higher compared with those in the untreated group (Fig. 3A). The results of RT-qPCR were similar to those in of western blotting (Fig. 3B). Cell beating was observed in ~15% BMSCs-Tbx18 at day 10 under a light microscope (magnification, x100, x200 and x400; Leica Microsystems GmbH). To further evaluate how G9a affected HCN4 expression, the enrichment of H3K9me2 in the HCN4 promoter was assessed. Compared with in the control group, H3K9me2 was significantly downregulated in the HCN4 promoter region following interference with G9a (Fig. 3C). These results demonstrated that G9a changed the enrichment level of H3K9me2 in the HCN4 promoter region, which suggested that H3K9me2 could regulate the expression of HCN4 and affect the formation of pacemaker-like cells through differential enrichment in the HCN4 promoter region.

Knocking down G9a promotes myocardial hypertrophy. The results of the *in vivo* study demonstrated that the heart volume and weight of rats were significantly increased following injection of BIX01294 compared with in the control group (P<0.05; Fig. 4A). H&E staining demonstrated that cardiomyocytes were hypertrophic and the nuclei were malformed in the treatment group (Fig. 4B). Immunohistochemical staining demonstrated that BIX01294 inhibited G9a, increased the protein expression levels of HCN4 in the sinoatrial node (Fig. 4B). Western blotting demonstrated that at day 50, the protein expression levels of H3K9me2 normalized to H3 were significantly decreased, whereas the protein expression levels of Nppa, Nppb and Myh7, indicators of cardiac hypertrophy, were significantly increased in the BIX01294 group compared with in the control group (Fig. 4D), which was consistent with their mRNA expression levels (P<0.05; Fig. 4C). These results demonstrated that interference with G9a *in vivo* increased proliferation of cardiomyocytes including the sinoatrial node cells.

Discussion

An ideal bio-pacemaker needs to have the same sustained, robust pacing ability as sinoatrial node cells. The generation methods of biological pacemakers in current studies mainly rely on making non-pacemaker cells possess the characteristics and functions of pacemaker cells while retaining their phenotypes. These methods can generate pacing current by regulating membrane potential or depolarization of cells; however, they have drawbacks, such as an unstable current, conduction block or lack of autonomous regulation. It was previously reported that *in vitro* and *in vivo*, both fibroblasts and quiescent cardiomyocytes transfected with the Tbx18 gene differentiated into sinoatrial node-like cells in phenotype and function (14). Moreover, HCN4, a key pacemaker gene, the

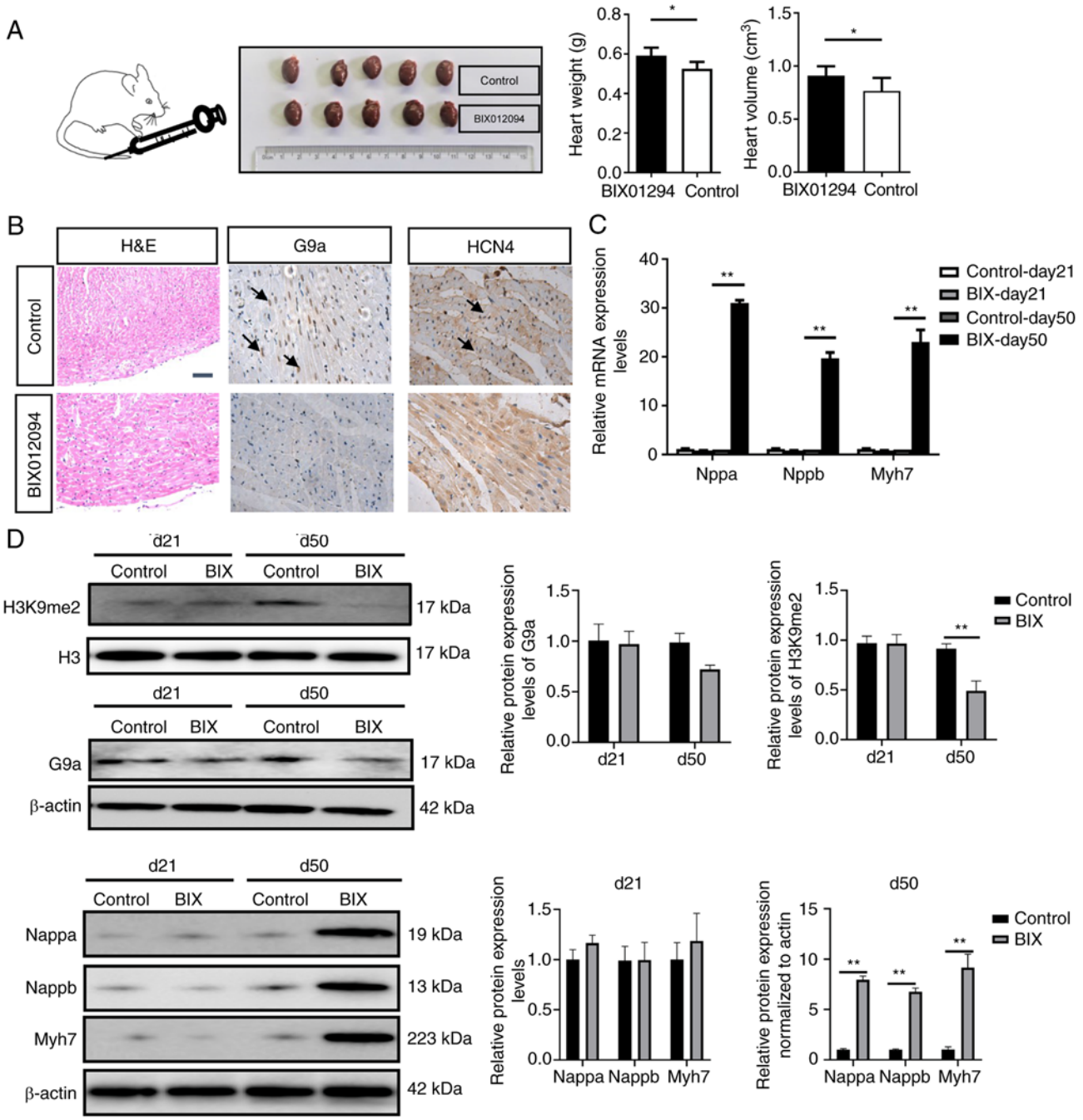

Figure 4. BIX01294 promotes cardiac hypertrophy. (A) BIX01294 was injected through the caudal vein, and heart volume and weight were assessed at day 50. (B) H&E staining of the heart and immunohistochemistry of sinoatrial node tissue. The arrow indicated positive cells. Scale bar, 50 μm. (C) Quantitative analysis of the mRNA expression levels of Nppa, Nppb and Myh7. (D) Western blotting was used to assess the protein expression levels of H3K9me2, G9a, Nppa, Nppb and Myh7. *P<0.05 and **P<0.01. H3K9me2, histone H3 at lysine 9 dimethylation; G9a, euchromatic histone lysine methyltransferase 2; H&E, haematoxylin and eosin; Nppa, natriuretic peptide A; Nppb, natriuretic peptide B; Myh7, myosin heavy chain 7.

expression levels of which were reported to be significantly upregulated after Tbx18 transduction, may be related to the formation of pacemaker-like cells (15,16). In the present study, through the overexpression of Tbx18, the mRNA and protein expression levels of HCN4 and the surface markers of cardiomyocytes were increased, which was consistent with previous reports (8,17,18). Moreover, it has been reported that Tbx18 transfection of neonatal rat myocardium not only increased the expression levels of HCN4, but also increased the frequency of spontaneous beating (5). These effects were reported to occur in cells at hyperpolarization due to the pacemaker current, which is driven by HCN protein (19). However, in the present study, beating was only demonstrated in ~5% of BMSCs-Tbx18 at day 10. The low efficiency on inducing cardiac differentiation of BMSCs was possibly due to the reduced response to other factors produced in the microenvironment that could be involved in the process of cardiac differentiation (20). Therefore, a method to improve the differentiation efficiency is required. It is well known that H3K9 is widely involved in cell proliferation and differentiation. Our previous study reported that knockdown of the histone methyltransferase G9a increased expression of early transcription factors during the

differentiation of MSCs into cardiomyocytes (21). BIX01294 was originally reported to be a G9a inhibitor during a chemical library screen of small molecules and has previously been used in the generation of induced pluripotent stem cells. It is reported to upregulate precardiac markers and allow bone marrow cells to respond to cardiogenic signals (22). Therefore, in the present study, H3K9me2 was significantly downregulated in the HCN4 promoter region following interference with G9a, which promoted HCN4 expression, thereby increasing the number of pacemaker-like cells and the beating of cells. *In vivo*, the reduction of microRNA-217 levels has been reported to reduce the expression of G9a, thereby promoting the reduction of H3K9me2 expression in the promoter region of Myh7, which resulted in pathological hypertrophy (9). In the present study, after BIX01294 injection, the cardiac volume and weight of rats significantly increased, as did certain indicators related to cardiac hypertrophy. The present study also demonstrated that the expression levels of HCN4 in the sinoatrial node increased after inhibition of G9a, which indicated that G9a was involved in the process of proliferation and the development of sinoatrial node cells.

The mechanism by which H3K9 is involved in the regulation of the differentiation of MSCs into cardiomyocytes is still unclear; however, it may be related to gene silencing by H3K9 methylation in the promoter region of genes (23,24). As the methylation modification enzyme of H3K9, G9a can catalyze single, double and trimethylation at H3K9 sites (25,26). The results of the present study demonstrated that interference with G9a could significantly reduce H3K9me2 protein expression levels. G9a can modify the H3K9 methylation of histones in certain gene promoter regions through its histone methyltransferases activity, thereby regulating gene transcriptional silencing (27). Therefore, as a substrate competition inhibitor, BIX01294 can be used to inhibit G9a to reverse transcriptional suppression of stem cell genes (28-30). Furthermore, it has previously been reported that BIX01294-pretreated human BMSCs can effectively differentiate into neuron-like cells by inducing the expression of neuronal-specific genes containing RE-1 sequences (31). The present study provided further functional verification, which demonstrated that interference with G9a could significantly downregulate the H3K9me2 enrichment level in the HCN4 promoter region. It may be hypothesized that the reduced enrichment of H3K9me2 in the HCN4 promoter region led to changes in chromosome state, promoted the binding of Tbx18 to the HCN4 promoter region and increased HCN4 transcription, which promoted cell differentiation to pacemaker-like cells. Furthermore, considering the complexity of the pacemaker-like cell formation process, further studies are needed, including to evaluate the effect of histone methylation modification on transcription factor formation in early cardiomyocytes to clarify the role of epigenetic modification in the formation of pacemaker-like cells.

In conclusion, the present study demonstrated that BIX01294 increased the differentiation efficiency of pacemaker-like cells by inhibiting the enrichment level of H3K9me2 in the HCN4 promoter region *in vitro* and *in vivo*. Therefore, using a G9a inhibitor such as BIX01294 may provide a better strategy for promoting stem cell differentiation into pacemaker-like cells. These results have important implications for regenerative medicine related to cellular therapy of chronic arrhythmias.

Acknowledgements

The authors would like to thank Professor Lei Sun (Cardiology Department, Northern Jiangsu People's Hospital, Yangzhou, China) for help with the experimental design.

Funding

This work was supported by a grant from Taizhou People's hospital (grant no. ZL202035).

Availability of data and materials

The datasets used and/or analyzed during the current study are available from the corresponding author on reasonable request.

Authors' contributions

PX, KJ, JZ, LD□JG□XG and XS were involved in the conception, design and implementation of the experimental plan, drafting the article and statistical analysis. PX and XS confirm the authenticity of all the raw data. All authors read and approved the final manuscript.

Ethics approval and consent to participate

All procedures involving the care and use of animals conformed to the Animal Research: Reporting of *In Vivo* Experiments guidelines and were approved by the Laboratory Animal Management and Experimental Animal Ethics Committee of Yangzhou University (approval no. 202003545).

Patient consent for publication

Not applicable.

Competing interests

The authors declare that they have no competing interests.

References

1. Sun X, Li H, Zhu Y, Xu P, Zuo Q, Li B and Gu X: 5-Azacytidine-induced cardiomyocyte differentiation of very small embryonic-like stem cells. Stem Cells Int 2020: 5162350, 2020.
2. Farraha M, Kumar S, Chong J, Cho HC and Kizana E: Gene therapy approaches to biological pacemakers. J Cardiovasc Dev Dis 5: 50, 2018.
3. Li Y, Yang M, Zhang G, Li L, Ye B, Huang C and Tang Y: Transcription factor TBX18 promotes adult rat bone mesenchymal stem cell differentiation to biological pacemaker cells. Int J Mol Med 41: 845-851, 2018.
4. Xiao H, Yang YJ, Lin YZ, Peng S, Lin S and Song ZY: Transcription factor Tbx18 induces the differentiation of c-kit^{+} canine mesenchymal stem cells (cMSCs) into SAN-like pacemaker cells in a co-culture model in vitro. Am J Transl Res 10: 2511-2528, 2018.
5. Gorabi AM, Hajighasemi S, Tafti HA, Atashi A, Soleimani M, Aghdami N, Saeid AK, Khori V, Panahi Y and Sahebkar A: TBX18 transcription factor overexpression in human-induced pluripotent stem cells increases their differentiation into pacemaker-like cells. J Cell Physiol 234: 1534-1546, 2019.

6. Wiese C, Grieskamp T, Airik R, Mommersteeg MT, Gardiwal A, de Gier-de Vries C, Schuster-Gossler K, Moorman AF, Kispert A and Christoffels VM: Formation of the sinus node head and differentiation of sinus node myocardium are independently regulated by Tbx18 and Tbx3. Circ Res 104: 388-397, 2009.
7. Szabo E, Rampalli S, Risueño RM, Schnerch A, Mitchell R, Fiebig-Comyn A, Levadoux-Martin M and Bhatia M: Direct conversion of human fibroblasts to multilineage blood progenitors. Nature 468: 521-526, 2010.
8. Hu Y, Li N, Liu L, Zhang H, Xue X, Shao X, Zhang Y and Lang X: Genetically modified porcine mesenchymal stem cells by lentiviral Tbx18 create a biological pacemaker. Stem Cells Int 2019: 3621314, 2019.
9. Thienpont B, Aronsen JM, Robinson EL, Okkenhaug H, Loche E, Ferrini A, Brien P, Alkass K, Tomasso A, Agrawal A, *et al*: The H3K9 dimethyltransferases EHMT1/2 protect against pathological cardiac hypertrophy. J Clin Invest 127: 335-348, 2017.
10. Livak KJ and Schmittgen TD: Analysis of relative gene expression data using real-time quantitative PCR and the 2(-Delta Delta C(T)) method. Methods 25: 402-408, 2001.
11. Kaur K, Yang J, Edwards JG, Eisenberg CA and Eisenberg LM: G9a histone methyltransferase inhibitor BIX01294 promotes expansion of adult cardiac progenitor cells without changing their phenotype or differentiation potential. Cell Prolif 49: 373-385, 2016.
12. Yang J, Kaur K, Edwards JG, Eisenberg CA and Eisenberg LM: Inhibition of histone methyltransferase, histone deacetylase, and β-catenin synergistically enhance the cardiac potential of bone marrow cells. Stem Cells Int 2017: 3464953, 2017.
13. Huang YL, Qiu RF, Mai WY, Kuang J, Cai XY, Dong YG, Hu YZ, Song YB, Cai AP and Jiang ZG: Effects of insulin-like growth factor-1 on the properties of mesenchymal stem cells in vitro. J Zhejiang Univ Sci B 13: 20-28, 2012.
14. Kapoor N, Liang W, Marbán E and Cho HC: Direct conversion of quiescent cardiomyocytes to pacemaker cells by expression of Tbx18. Nat Biotechnol 31: 54-62, 2012.
15. Schweizer PA, Darche FF, Ullrich ND, Geschwill P, Greber B, Rivinius R, Seyler C, Müller-Decker K, Draguhn A, Utikal J, *et al*: Subtype-specific differentiation of cardiac pacemaker cell clusters from human induced pluripotent stem cells. Stem Cell Res Ther 8: 229, 2017.
16. Chen L, Deng ZJ, Zhou JS, Ji RJ, Zhang X, Zhang CS, Li YQ and Yang XQ: Tbx18-dependent differentiation of brown adipose tissue-derived stem cells toward cardiac pacemaker cells. Mol Cell Biochem 433: 61-77, 2017.
17. Wang F, Zhao H, Yin L, Tang Y, Wang X, Zhao Q, Wang T and Huang C: Transcription factor TBX18 reprograms vascular smooth muscle cells of ascending aorta to pacemaker-like cells. DNA Cell Biol 38: 1470-1479, 2019.
18. Wu L, Du J, Jing X, Yan Y, Deng S and Hao Z: Bone morphogenetic protein 4 promotes the differentiation of Tbx18-positive epicardial progenitor cells to pacemaker-like cells. Exp Ther Med 17: 2648-2656, 2019.
19. DiFrancesco D: The role of the funny current in pacemaker activity. Circ Res 106: 434-446, 2010.
20. Yang G, Tian J, Feng C, Zhao LL, Liu Z and Zhu J: Trichostatin a promotes cardiomyocyte differentiation of rat mesenchymal stem cells after 5-azacytidine induction or during coculture with neonatal cardiomyocytes via a mechanism independent of histone deacetylase inhibition. Cell Transplant 21: 985-996, 2012.
21. Sun X, Gu X, Li H, Xu P, Li M, Zhu Y, Zuo Q and Li B: H3K9me2 regulates early transcription factors to promote mesenchymal stem-cell differentiation into cardiomyocytes. Mol Med Rep 24: 616, 2021.
22. Hayes M and Zavazava N: Strategies to generate induced pluripotent stem cells. Methods Mol Biol 1029: 77-92, 2013.
23. Snowden AW, Gregory PD, Case CC and Pabo CO: Gene-specific targeting of H3K9 methylation is sufficient for initiating repression in vivo. Curr Biol 12: 2159-2166, 2002.
24. Sasidharan Nair V, El Salhat H, Taha RZ, John A, Ali BR and Elkord E: DNA methylation and repressive H3K9 and H3K27 trimethylation in the promoter regions of PD-1, CTLA-4, TIM-3, LAG-3, TIGIT, and PD-L1 genes in human primary breast cancer. Clin Epigenetics 10: 78, 2018.
25. Collins RE, Tachibana M, Tamaru H, Smith KM, Jia D, Zhang X, Selker EU, Shinkai Y and Cheng X: In vitro and in vivo analyses of a Phe/Tyr switch controlling product specificity of histone lysine methyltransferases. J Biol Chem 280: 5563-5570, 2005.
26. Kubicek S, O'Sullivan RJ, August EM, Hickey ER, Zhang Q, Teodoro ML, Rea S, Mechtler K, Kowalski JA, Homon CA, *et al*: Reversal of H3K9me2 by a small-molecule inhibitor for the G9a histone methyltransferase. Mol Cell 25: 473-481, 2007.
27. Son HJ, Kim JY, Hahn Y and Seo SB: Negative regulation of JAK2 by H3K9 methyltransferase G9a in leukemia. Mol Cell Biol 32: 3681-3694, 2012.
28. Yang J, Kaur K, Ong LL, Eisenberg CA and Eisenberg LM: Inhibition of G9a histone methyltransferase converts bone marrow mesenchymal stem cells to cardiac competent progenitors. Stem Cells Int 2015: 270428, 2015.
29. Hou P, Li Y, Zhang X, Liu C, Guan J, Li H, Zhao T, Ye J, Yang W, Liu K, *et al*: Pluripotent stem cells induced from mouse somatic cells by small-molecule compounds. Science 341: 651-654, 2013.
30. Kim HT, Jeong SG and Cho GW: G9a inhibition promotes neuronal differentiation of human bone marrow mesenchymal stem cells through the transcriptional induction of RE-1 containing neuronal specific genes. Neurochem Int 96: 77-83, 2016.
31. Mezentseva NV, Yang J, Kaur K, Iaffaldano G, Rémond MC, Eisenberg CA and Eisenberg LM: The histone methyltransferase inhibitor BIX01294 enhances the cardiac potential of bone marrow cells. Stem Cells Dev 22: 654-667, 2013.

This work is licensed under a Creative Commons Attribution-NonCommercial-NoDerivatives 4.0 International (CC BY-NC-ND 4.0) License.